

CONF-961245--2

**Analysis and Performance of Adjacent-Cell Preconditioners for
Accelerating Multidimensional Transport Calculations***

Y. Y. Azmy

Oak Ridge National Laboratory**
Oak Ridge, Tennessee 37831-6363

"The submitted manuscript has been authored by a contractor of the U. S. Government under contract No. DE-AC05-96OR22464. Accordingly, the U.S. Government retains a nonexclusive, royalty-free license to publish or reproduce the published form of this contribution, or allow others to do so, for U.S. Government purposes."

RECEIVED

DEC 31 1996

OSTI

MASTER

to be presented at the
OECD/NEA meeting on 3D Deterministic Radiation Transport Computer Programs,
Feature, Applications and Perspectives
Paris, France
December 2-3, 1996

* Research sponsored by the U.S. Department of Energy.

**Managed by Lockheed Martin Energy Research Corp. for the U. S. Department of Energy under
Contract DE-AC05-96OR22464.

DISTRIBUTION OF THIS DOCUMENT IS UNLIMITED

Um

DISCLAIMER

This report was prepared as an account of work sponsored by an agency of the United States Government. Neither the United States Government nor any agency thereof, nor any of their employees, makes any warranty, express or implied, or assumes any legal liability or responsibility for the accuracy, completeness, or usefulness of any information, apparatus, product, or process disclosed, or represents that its use would not infringe privately owned rights. Reference herein to any specific commercial product, process, or service by trade name, trademark, manufacturer, or otherwise does not necessarily constitute or imply its endorsement, recommendation, or favoring by the United States Government or any agency thereof. The views and opinions of authors expressed herein do not necessarily state or reflect those of the United States Government or any agency thereof.

DISCLAIMER

**Portions of this document may be illegible
in electronic image products. Images are
produced from the best available original
document.**

ANALYSIS AND PERFORMANCE OF ADJACENT-CELL PRECONDITIONERS FOR ACCELERATING MULTIDIMENSIONAL TRANSPORT CALCULATIONS*

Y. Y. Azmy
Oak Ridge National Laboratory
P.O. Box 2008, MS 6363
Oak Ridge, TN 37831

Abstract

The formal development of the Adjacent-cell Preconditioner (AP) and its implementation in the TORT code are briefly reviewed. Based on earlier experience with diffusion type acceleration, and excellent results in slab geometry the reciprocal averaging formula is used to mix the preconditioner elements across material and mesh discontinuities. Numerical testing of the method employing the Burre Suite of Test Problems (BSTeP), a collection of 144 cases covering a wide range in parameter space, using AP, Partial Current Rebalance (PCR), and TWODANT's Diffusion Synthetic Acceleration (DSA) is presented. While AP outperforms the other two methods for the majority of the cases included in BSTeP it consumes many more iterations than can be explained by spectral analysis of the homogeneous model problem in cases with sharp material discontinuity. In order to verify this undesirable behavior and explore potential remedies a model problem, the Periodic Horizontal Interface (PHI), is developed that permits discontinuity of nuclear properties and cell height across the interface. Fourier mode decomposition is applied to AP with the reciprocal averaging mixing formula for the PHI configuration and shown to possess a spectral radius that approaches unity as the material discontinuity gets larger. The question of whether an unconditionally stable AP exists for PHI is tackled and preliminary indications are negative. Novel preconditioners that have nontraditional cell-coupling schemes that remain stable in these regimes may have to be sought.

Introduction

It has been well known for many years that the iterative scheme used to solve the discrete ordinates approximation of the transport equation using a wide variety of spatial approximations slows down considerably in problems that do not sufficiently dissipate neutrons by leakage or removal. Classical methods such as rebalance schemes¹ improved the rate of convergence in many cases but still failed in others. Using a diffusion computation to accelerate convergence of the transport solution,² Diffusion Synthetic Acceleration (DSA), also produced mixed results, but was generally judged inadequate especially for the Diamond Difference (DD) method.³ Further insight into the

Managed by Lockheed Martin Energy Research, Inc. under contract DE-AC05-96OR22464 with the U.S. Department of Energy.

behavior of DSA was articulated in Alcouffe's consistency principle,⁴ and formalized by Larsen's Four-Step Method,⁵ based on the premise that the diffusion operator must be *consistent* with the discrete variable transport operator. This turns out to be a severely restrictive requirement for large production codes because it amounts to an edge-centered diffusion coupling scheme that, for all methods but DD, results in a very large system of equations in multidimensional geometry. It was later shown,⁶ however, that cell-centered diffusion operators can effectively accelerate transport calculations based on spatial approximations of the general Weighted Diamond Difference (WDD) form if the spatial weights are sufficiently large for thick cells.

The Adjacent-cell Preconditioner (AP) method is founded on this result, namely that it is possible to construct a cell-centered preconditioner for the mesh sweep that bounds the spectral radius of the entire iterative process far below unity. In slab geometry AP was shown to exhibit excellent spectral properties consistent with the spectral analysis of the homogeneous material, uniform mesh model problem, even for test problems with a non-uniform mesh and material heterogeneities.⁷ The extension of AP to multidimensional Cartesian geometry possessed similar spectral properties for model problems, but testing with problems in which material heterogeneity and non-uniform mesh are permitted showed a significant increase in the spectral radius.⁸

The purpose of this paper is two fold. First we will verify the deterioration in spectral properties of AP when combined with reciprocal averaging to treat heterogeneities via a new model problem, Periodic Horizontal Interface (PHI). Then we will attempt to optimize the AP elements to minimize the spectral radius and conclude that this value approaches unity as the computational cell aspect ratio approaches 0 and the material discontinuity increases.

In the next section we review the AP formalism for multidimensional Cartesian geometry. Then we discuss its implementation into the TORT code, and demonstrate its efficiency compared to other acceleration schemes, like TORT's Partial Current Rebalance (PCR),¹ and TWODANT's DSA,⁹ via the Burre Suite of Test Problems (BSTeP).⁸ Next the discrepancy between the rate of convergence of some of the BSTeP cases and the spectral analysis leads us to formulate the PHI configuration and to investigate its spectral properties as a function of problem parameters. We close with a brief summary and our conclusions.

The Adjacent-cell Preconditioning Formalism

The AP formalism is based on a Fourier decomposition of the *linear* iterative operator comprised of the mesh sweep stage and the preconditioning stage into eigenmodes. This is performed in the usual homogeneous model problem setting for an arbitrary preconditioner that couples each computational cell to itself and its adjacent neighbors, the standard cell-centered diffusion stencil. However, in AP the preconditioner elements are not based on the diffusive properties of the computational cells involved, e.g. diffusion length. Rather, for a generic WDD method they are determined by requiring: (a) the eigenvalue of the combined mesh sweep-AP iterations to vanish in the vicinity of the origin in Fourier space; and (b) the diagonal and off-diagonal elements of the preconditioner to satisfy a diffusion-like condition.^{7,8} The latter is equivalent to requiring the preconditioner to become singular at the origin in Fourier space for perfectly scattering materials so that convergence of the *flattest* eigenmode is determined by the spectrum in this limit.

The AP formalism starts with the WDD form of the discrete-variable transport equation in two-dimensional Cartesian geometry comprised of a balance equation,

$$\frac{\epsilon_j^x}{2} (\psi_{+j}^y - \psi_{-j}^y) + \frac{\epsilon_j^y}{2} (\psi_{+j}^x - \psi_{-j}^x) + \bar{\psi}_j = c_j \bar{\phi}_j^l, \quad (1)$$

and one weighted difference relation per dimension,

$$\bar{\psi}_j = \left[\frac{1 + \alpha_j^x}{2} \right] \psi_{+j}^y + \left[\frac{1 - \alpha_j^x}{2} \right] \psi_{-j}^y, \quad (2)$$

with an analogous expression in the y -dimension. [Extension to three-dimensional Cartesian geometry is straightforward]. In Eqs. (1,2) ψ_{+j}^y , and ψ_{-j}^y are the y -averaged angular flux on the outgoing, and incoming $x=const$ edges of a generic cell of type j , respectively; ψ_{+j}^x and ψ_{-j}^x are defined analogously; $\bar{\psi}_j$, and $\bar{\phi}_j^l$ are the cell-averaged angular flux, and the previous iterate of the scalar flux in a generic cell of type j , respectively. The type of the cell essentially refers to its material composition and geometry, i.e. σ_j, c_j, a_j, b_j is the total cross section, scattering ratio, width, and height of cell type j , respectively. It is worth noting that we write Eq. (1) in the *mathematically* homogeneous, i.e. source free, form for the purpose of the Fourier analysis discussed shortly; in normal form the right hand side of Eq. (1) includes the average of the volumetric source over the cell. Also in Eq. (1) we have defined,

$$\epsilon_j^x \equiv 2 |\mu| / (\sigma_j a), \quad (3)$$

and its y -analogue. The spatial weights in Eq. (2) typically satisfy $\alpha_j^x, \alpha_j^y \in [0,1]$; for example the Zero-order Nodal Integral Method (ONIM) corresponds to,

$$\alpha_j^x \equiv \coth(1/\epsilon_j^x) - \epsilon_j^x, \quad (4)$$

with an analogous expression in the y -dimension, which correctly approaches the DD limit of 0, and Step limit of 1, for thin, and thick cells, respectively. Note that in Eqs. (1,2) the discrete ordinate and iteration indices on the angular flux discrete variables, and in Eqs. (3,4) the discrete ordinate index on angle dependent parameters, have been suppressed for clarity's sake.

The current iterate of the scalar flux is computed from,

$$\bar{\phi}_j^l = \sum_{\mu, \eta} \omega \bar{\psi}_j, \quad (5)$$

where ω is the angular weight associated with the discrete ordinate (μ, η) . Convergence of the iterative process l is characterized by the largest magnitude relative difference between $\bar{\phi}_j^l$ and $\bar{\phi}_j^{l-1}$ over all computational cells comprising a given problem. In the Source Iterations (SI) the new iterate of the scalar flux is set to the current iterate but typically an acceleration scheme is implemented to compute an improved new iterate from $\bar{\phi}_j^l$. A general framework for this process is provided by AP whereby an arbitrary preconditioner, \mathbf{D} , is applied to the iterates,

$$\bar{\phi}_j^{l+1} = \bar{\phi}_j^l + \mathbf{D}^{-1} (\bar{\phi}_j^l - \bar{\phi}_j^{l-1}). \quad (6)$$

For example the SI are obtained by setting $\mathbf{D} = \mathbf{I}$, where \mathbf{I} is the identity matrix. It is important to notice that \mathbf{D} is a cell-centered operator, distinguishing the AP formalism from consistent DSA schemes strictly based on Larsen's method.⁵

Decomposing Eqs. (1,2,5,6) into Fourier modes and applying the AP conditions described above yields the preconditioner elements coupling each computational cell to its neighbors in the x -dimension,

$$D_{xj}^H \equiv -\frac{1}{4c_j} \sum_{\mu, \eta} \omega \epsilon_j^x (\epsilon_j^x + \alpha_j^x), \quad (7)$$

with an analogous expression in the y -dimension. The superscript H in Eq. (7) indicates that this expression is based on the spectral analysis of the homogeneous model problem.

The spectra of the resulting iterations for a wide range of problem parameters exhibit a spectral radius smaller than .25, that vanishes (implying immediate convergence) for very thick computational cells. More importantly, unlike other unconditionally stable acceleration schemes, the AP is cell-centered and its spectral radius remains small when the cell aspect ratio approaches 0 or ∞ .

This completes our brief review of the AP formalism. Details, as well as performance analysis for homogeneous model problem settings have been presented in Ref. 8.

Implementation in TORT and Numerical Tests

Implementation of the AP requires supplying expressions for the standard types of boundary conditions, as well as a mixing formula for the preconditioner elements across material discontinuities and mesh non-uniformities. The boundary conditions are based on Larsen's prescription⁵ adapted to multidimensional geometry; the interested reader should consult Ref. 8 for details. In light of the close resemblance between the AP operator and standard cell-centered diffusion operators, and given the good results achieved in slab geometry,⁷ the reciprocal-averaging formula was employed in the multidimensional implementation of AP.⁸ More explicitly, this amounts to computing each cell's AP coefficients using the homogeneous model problem formulas, Eq. (7), then setting the preconditioner element coupling horizontally adjacent cells type j and k to,

$$D_{xj} \equiv \frac{2 \sigma_k a_k}{\sigma_k a_k / D_{xj}^H + \sigma_j a_j / D_{xk}^H} , \quad (8)$$

This provides the preconditioner elements coupling each cell to its adjacent neighbors; applying the stability condition derived earlier⁸ produces an expression for the self-coupling elements of the preconditioner,

$$D_j = \frac{1}{c_j} - 1 - 2D_{xj} - 2D_{yj} . \quad (9)$$

The AP equations presented above were implemented in TORT to accelerate a special linear form of the θ -Weighted scheme, as well as other flux approximation methods. In order to test the performance of AP over a range in parameter space that includes cases of sharp material discontinuity and mesh non-uniformity we employed BSTeP.⁸ The geometric configuration and nuclear properties of this suite of 144 test problems has been published earlier.⁸ As a motivation for the PHI analysis presented in the next section, to illustrate its relevance to other acceleration schemes, and to demonstrate the superior efficiency of AP in general we present in Table 1 a comparison of the number of iterations required to achieve 10^{-4} relative convergence for BSTeP by three methods. These are the AP and PCR for the Step method as implemented in a special version of TORT, and TWODANT's DSA for the Adaptive DD.⁹

Overall AP converges more rapidly than the other two methods shown in Table 1. However, its rate of convergence deteriorates significantly for BSTeP cases with large material discontinuities. While the number of AP iterations for such cases is far fewer than unaccelerated iterations, and generally fewer than the number of PCR iterations in TORT,¹ and than DSA iterations in TWODANT,⁹ among others, it consumed many more iterations than predicted by the spectral analysis. Understanding this phenomenon is essential to finding a remedy, if one exists, or pursuing alternative preconditioners otherwise.

Periodic Horizontal Interface Configuration Spectral Analysis

Three potential sources for the discrepancy between the spectral analysis of the homogeneous model problem and the observed rate of convergence in the numerical experiments described in the previous section have been identified. First, is the boundary conditions; good agreement between the spectral analysis and numerical experiments with homogeneous problem configurations of finite

Table 1. Number of Iterations Required to Achieve Convergence for BSTeP Using the Symmetric AP (top), TORT's Rebalance (middle), for the Step Method in a Special Version of TORT, and DSA (bottom) for Adaptive DD in TWODANT 3.0, on IBM RS6000.

		σ_1												
		.01			.1			1			10			
		dy ₁	.01	.1	1	.01	.1	1	.01	.1	1	.01	.1	1
σ_2	.01	dy ₂	7	5	5	8	7	7	10	13	9	24	32	13
		.01	4	5	5	6	7	10	9	13	18	19	58	55
			15†	6†	5	16†	9†	6†	15†	16†	13	48†	259†	500
	.1	.1	5	5	5	8	7	8	12	13	15	15	28	21
			5	5	5	5	6	10	11	12	17	17	26	149
			6†	5†	5	8†	8	7	15†	15†	21	168†	474†	500
	1	1	5	5	5	8	8	8	12	12	12	13	14	12
			5	5	5	8	6	10	13	12	13	106	59	108
			5	5	5	7	7†	8	12†	14	15	246†	255	42
.1	.01	8	6	5	8	7	7	8	7	7	14	12	6	
		5	5	5	6	7	10	9	13	18	18	53	53	
		18†	6†	5	14†	8†	6	13†	10†	6	60†	241†	233	
.1	.1	7	6	5	7	7	7	9	8	8	10	14	9	
		5	6	5	7	7	10	13	11	28	15	55	143	
		8†	8†	5	8†	7†	6	7†	10	8	39†	165†	43	
1	1	7	7	7	6	6	7	10	10	9	9	11	9	
		8	8	6	8	8	11	13	15	12	76	59	72	
		6†	6†	7	6	6†	7	8†	10	10	443	125	404†	
10	.01	.01	13	8	5	9	7	7	7	8	7	10	6	5
			6	5	5	6	6	10	8	12	17	17	35	49
			16†	9†	5	13†	9†	6†	10†	9†	6	39†	231†	308
	.1	.1	11	14	10	8	9	8	8	8	7	9	7	6
			9	11	8	8	11	8	15	9	13	32	37	114
			8†	8†	7†	11†	14†	9	9	10†	6	22	335†	204
	1	1	9	10	13	8	8	8	8	8	8	8	7	6
			11	10	9	9	10	13	9	8	10	72	77	59
			7†	29†	14	18	11†	9†	8	8†	6	217†	500	500
.01	.01	32	17	11	17	12	9	7	8	7	10	8	6	
		12	10	9	12	10	7	11	17	16	13	25	43	
		18†	19†	11	25†	18†	9†	20†	15†	8	54†	148†	274	
.1	.1	24	19	13	9	11	9	8	9	8	8	9	7	
		18	13	12	23	13	9	14	15	21	16	16	18	
		60†	67†	23	50†	43†	18	55†	40†	18	162†	265†	500	
1	1	12	12	8	8	8	8	8	9	8	8	8	5	
		18	20	18	23	16	13	12	21	22	47	17	19	
		71†	67†	60	71†	65†	54†	106†	89†	40†	500	500	500	

DSA: 500 ⇒ not converged

† Faster convergence obtained with $w_{damp}=2.0$

extent lead us to eliminate this possibility. Second, is implementation bugs or artificial numerical imprecision effects; we established the PHI problem configuration to show in this section that this phenomenon is genuine. Third, is the mixing formula across material discontinuities; again we use PHI in conjunction with an optimization library routine to demonstrate that no AP exists that results in an unconditionally stable and robust iterative procedure.

The PHI configuration is comprised of two types, $j = 1, 2$, of infinite horizontal stripes one cell thick each, stacked on top of one another so that every stripe of type 1(2) is sandwiched between two stripes of type 2(1), respectively. Thus the horizontal interface separating stripe types 1 and 2 repeats periodically along the y -dimension. The WDD equations for PHI are comprised of two sets of equations each including Eqs. (1), (2), and its y -analogue, for stripe type $j = 1, 2$. Using the continuity of the angular flux across the horizontal interface it can be eliminated from the combined set of equations described above. Introducing a Fourier mode decomposition of all dependent variables in the resulting equations yields a mapping of the eigenmode of the present iterate of the scalar flux, $\{\bar{\Phi}_1^i, \bar{\Phi}_2^i\}^T$, into the eigenmodes of the mesh-sweep scalar flux, $\{\tilde{\Phi}_1^i, \tilde{\Phi}_2^i\}^T$, that is governed by,

$$\begin{bmatrix} \tilde{\Phi}_1^i \\ \tilde{\Phi}_2^i \end{bmatrix} = \mathbf{B} \begin{bmatrix} \bar{\Phi}_1^i \\ \bar{\Phi}_2^i \end{bmatrix}, \quad (10)$$

where,

$$\mathbf{B} \equiv \sum_{\mu, \eta} \omega \mathbf{A}^{-1} \mathbf{C}, \quad (11.a)$$

$$\mathbf{A} = \mathbf{I} + \frac{\hat{\imath} \operatorname{sg}(\mu) \sin r}{\cos r + \hat{\imath} \operatorname{sg}(\mu) \alpha_1^x \sin r} \begin{bmatrix} \epsilon_1^x & 0 \\ 0 & \epsilon_2^x \end{bmatrix} + \frac{1}{(\alpha_1^y + \alpha_2^y) \cos s + \hat{\imath} \operatorname{sg}(\eta) (1 + \alpha_1^y \alpha_2^y) \sin s} \\ \times \begin{bmatrix} \epsilon_1^y (\cos s + \hat{\imath} \operatorname{sg}(\eta) \alpha_2^y \sin s) & -\epsilon_2^y \\ -\epsilon_2^y & \epsilon_1^y (\cos s + \hat{\imath} \operatorname{sg}(\eta) \alpha_2^y \sin s) \end{bmatrix}, \quad (11.b)$$

$$\mathbf{C} = \begin{bmatrix} c_1 & 0 \\ 0 & c_2 \end{bmatrix}. \quad (11.c)$$

In Eqs. (11) we defined $\hat{\imath} \equiv \sqrt{-1}$, $\operatorname{sg}(\cdot)$ is the signum function, and $r \equiv \lambda_x a/2$, $s \equiv \lambda_y (b_1 + b_2)/2$, where λ_x, λ_y are the Fourier variables in the x, y -dimensions, respectively.

Since \mathbf{B} is a 2×2 matrix it has in general two eigenmodes at each point in Fourier space represented by (r, s) . The spectral radius of the SI scheme then corresponds to the supremum of the absolute value of the eigenvalues of \mathbf{B} over the Fourier space. Similar to the homogeneous model problem spectral analysis, here also the spectral radius is unity, and slowest converging modes are the *flattest* modes with $r, s \rightarrow 0$. One interesting feature of the PHI analysis spectra is the diminishing range of the eigenvalues in cases with at least one optically thick stripe. This implies that eigenvalues for a finite problem configuration will be closer to one another thus reducing the dominance ratio of the fundamental mode and slowing down convergence in a way characterized by an initial linear increase in the error prior to the onset of exponential decay. This type of behavior of the iteration error has indeed been observed in numerical experiments.

The AP prescription for the coupling scheme among the computational cells is similar to the cell-centered diffusion stencil which when decomposed into Fourier modes produces,

$$\mathbf{D} \begin{bmatrix} \bar{\Phi}_1 \\ \bar{\Phi}_2 \end{bmatrix} = \begin{bmatrix} D_1 + 2D_{x1} \cos(2r) & 2D_{y1} \cos(s) \\ 2D_{y2} \cos(s) & D_2 + 2D_{x2} \cos(2r) \end{bmatrix} \begin{bmatrix} \bar{\Phi}_1 \\ \bar{\Phi}_2 \end{bmatrix}, \quad (12)$$

where D_1, D_2 are the self-coupling elements of \mathbf{D} for cells in stripes 1, 2, respectively; D_{x1}, D_{x2} are the coupling elements in the x -dimension for each stripe type; and D_{y1}, D_{y2} are the elements coupling the scalar flux in cells type 1 (2) to its value in cells type 2 (1) in the y -dimension, respectively. As expected, if the preconditioner elements are real, then the operator \mathbf{D} is real and periodic. The elements of the preconditioner in Eq. (12) have been intentionally left unspecified to stress the fact that a substantial degree of freedom is permitted in selecting them, as is done shortly in optimizing the spectral radius. However, if reciprocal averaging of the homogeneous model problem preconditioner elements is adopted then the elements of \mathbf{D} for PHI are given by Eqs. (8,9).

Decomposing the updating formula, Eq. (6), into Fourier modes, and using Eqs. (10) and (12) we obtain,

$$\bar{\Phi}^{l+1} = \mathbf{M} \bar{\Phi}^l \quad (13)$$

where we have defined,

$$\bar{\Phi}^v \equiv \{\bar{\Phi}_1^v, \bar{\Phi}_2^v\}^T, \quad v=l, l+1, \quad (14.a)$$

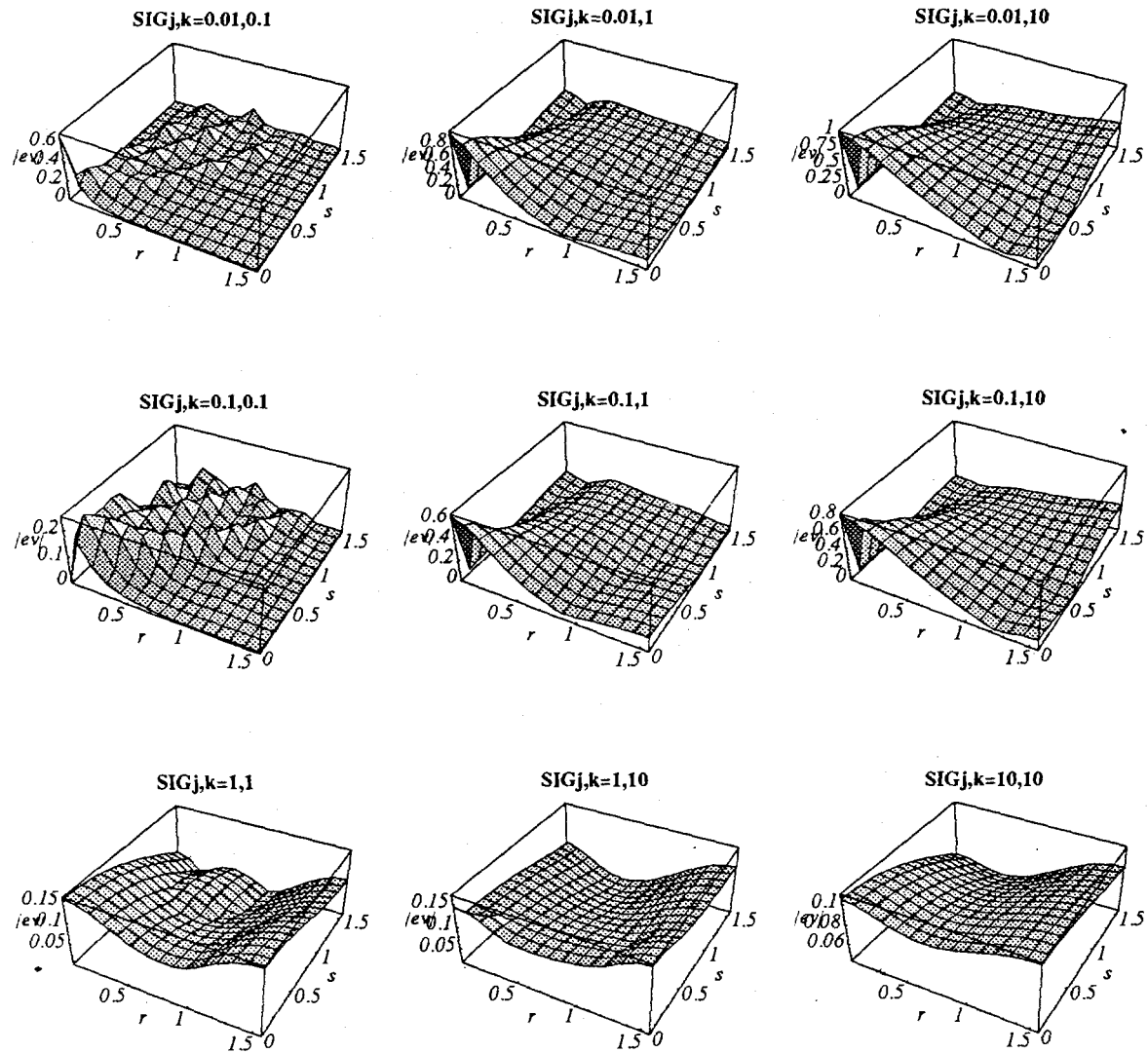
$$\mathbf{M} \equiv \mathbf{B} + \mathbf{D}^{-1}(\mathbf{B}-\mathbf{I}). \quad (14.b)$$

The spectrum of the matrix \mathbf{M} determines the eigenmodes of the AP iterative process for the PHI configuration. Sample plots of the largest magnitude (among two) eigenvalue of the AP with reciprocal averaging for the PHI configuration over the Fourier plane are depicted in Fig. 1 for ONIM with S_4 angular quadrature, $\mathbf{C}=\mathbf{I}$, $a=b_1=b_2=1$, and a range of total cross sections.

In general the spectra shown in Fig. 1 exhibit an improvement over the SI scheme particularly in cases where the material, i.e. total cross section, discontinuity is not too large. Nevertheless, these plots confirm the numerically observed increase in the spectral radius, approaching unity as the material discontinuity gets sharper thus implying increasing number of iterations to achieve convergence. Two features of the eigenvalues presented in Fig. 1 are worth noting. First, unlike the homogeneous model problem configuration where Eqs. (7) guarantee the vanishing of the eigenvalue corresponding to the $r=0=s$ mode, the PHI configuration eigenvalues generally do not approach zero around the origin in Fourier space even in the homogeneous cases $\sigma_j = \sigma_k$. This is due to the fact that in the PHI analysis where a cell-couple is considered simultaneously the *flat* eigenmode, i.e. $\bar{\Phi}_1^l = \bar{\Phi}_2^l$, involves two of the homogeneous model problem eigenmodes: $r=0=s$ and $r=0, s=-(b_1+b_2)/2$ modes. The latter mode's eigenvalue is not necessarily zero by the choice of the preconditioner, Eq. (8,9), and since the largest magnitude eigenvalue is plotted in Fig. 1 it always dominates the zero eigenvalue corresponding to the former mode. Second, the largest magnitude eigenvalue surface undergoes a sharp discontinuity especially when one of the stripe types is optically thin and the other thick. In particular, the eigenvalue appears to vanish as $s \rightarrow 0$ but approaches a finite value, whose magnitude goes to 1 as the total cross section discontinuity increases, as $r \rightarrow 0$.

The deterioration in the spectral properties of AP combined with the reciprocal averaging inspired several attempts to construct a preconditioner that is unconditionally stable and robust for the PHI configuration. Among these was a preconditioner that produces a vanishing eigenvalue along the trajectory $r=s \rightarrow 0$, another provided a continuous eigensurface near the origin. The failure of all such attempts raises an important question. Is there any preconditioner with the adjacent-cell coupling stencil that is unconditionally stable and robust? We explore this question with the following two caveats. First, we limit our search at this stage to the PHI configuration. Clearly if the answer to the posed question is negative for PHI then unconditional stability is unattainable in general and we terminate the search. On the other hand if we succeed in finding a mixing formula that renders AP unconditionally stable for PHI we must then extend and test it to general problem configurations with material discontinuities that are multidimensional in nature. Second, we conduct the search using NETLIB's *subplex* subroutine which implements the

Fig. 1. Largest Magnitude Eigenvalue of the AP with Reciprocal Averaging for the PHI Configuration for ONIM with S_4 Angular Quadrature, $C=I$, $a=b_1=b_2=1$, and $\sigma_1, \sigma_2 \in [.01, 10]$.



subspace-searching simplex method for the unconstrained optimization of general multivariate functions.¹⁰ Not only are optimization methods incapable of producing global extremal points in general, in this case roundoff errors due to finite arithmetic precision give rise to fictitious local minima that must be identified as such before reaching a conclusion.

The optimization process is performed by allowing *subplex* to modify the four preconditioner elements $D_{x_j} D_{y_j}$, $j=1,2$, then compute the self-coupling elements from the stability condition, Eq. (9). For each selection of the AP coefficients the AP-iteration eigenvalues are computed over a grid in Fourier space and the largest magnitude eigenvalue is assumed to represent the spectral radius, the objective function to be minimized by *subplex*. Typically several hundred evaluations of the objective function are needed to produce a minimum. In order to visually verify the resulting

optimal preconditioner we generate a gray-scale plot of the spectral radius at the computed values of D_{yj} over the D_{xj} plane.

Applying this strategy to the case shown in Fig. 1 with $\sigma_j = .01, 10$ and using the initial guess $D_{xj} = -100, -.01, D_{yj} = -10, -.01$ produces the optimal spectral radius of .33 with the preconditioner $D_{xj} = -74.14, -.02311, D_{yj} = -38.35, -.04727$, a very good result. Repeating the process for the case with $b_1 = .01 = b_2$, the initial guess $D_{xj} = -10, -.1, D_{yj} = -1000, -100$ yields the smallest spectral radius of .86 at $D_{xj} = -8.000, -.1000, D_{yj} = -28752, -596.6$. A gray-scale plot of the spectral radius over the D_{xj} plane for the optimal values of D_{yj} is depicted in Fig. 2. The apparent ragged behavior of the spectral radius surface in the upper right quadrant of the plot we conjecture is due to numerical imprecision effects. The two important features of Fig. 2 are: the large value of the optimal spectral radius, and the clearly defined relationship of the optimal values of D_{xj} , namely linear.

In order to test the first feature further, we increased the material discontinuity to $\sigma_1 = .001, \sigma_2 = 100$ and started the optimization process from $D_{xj} = -1, -.1, D_{yj} = -1000, -.1$ to obtain the smallest spectral radius of .98 at $D_{xj} = -5.987, -.09650, D_{yj} = -62.50, -4814$. Extrapolating the smallest spectral radius obtained to even larger material discontinuities leads us to conjecture that there is no cell-centered AP that is unconditionally stable.

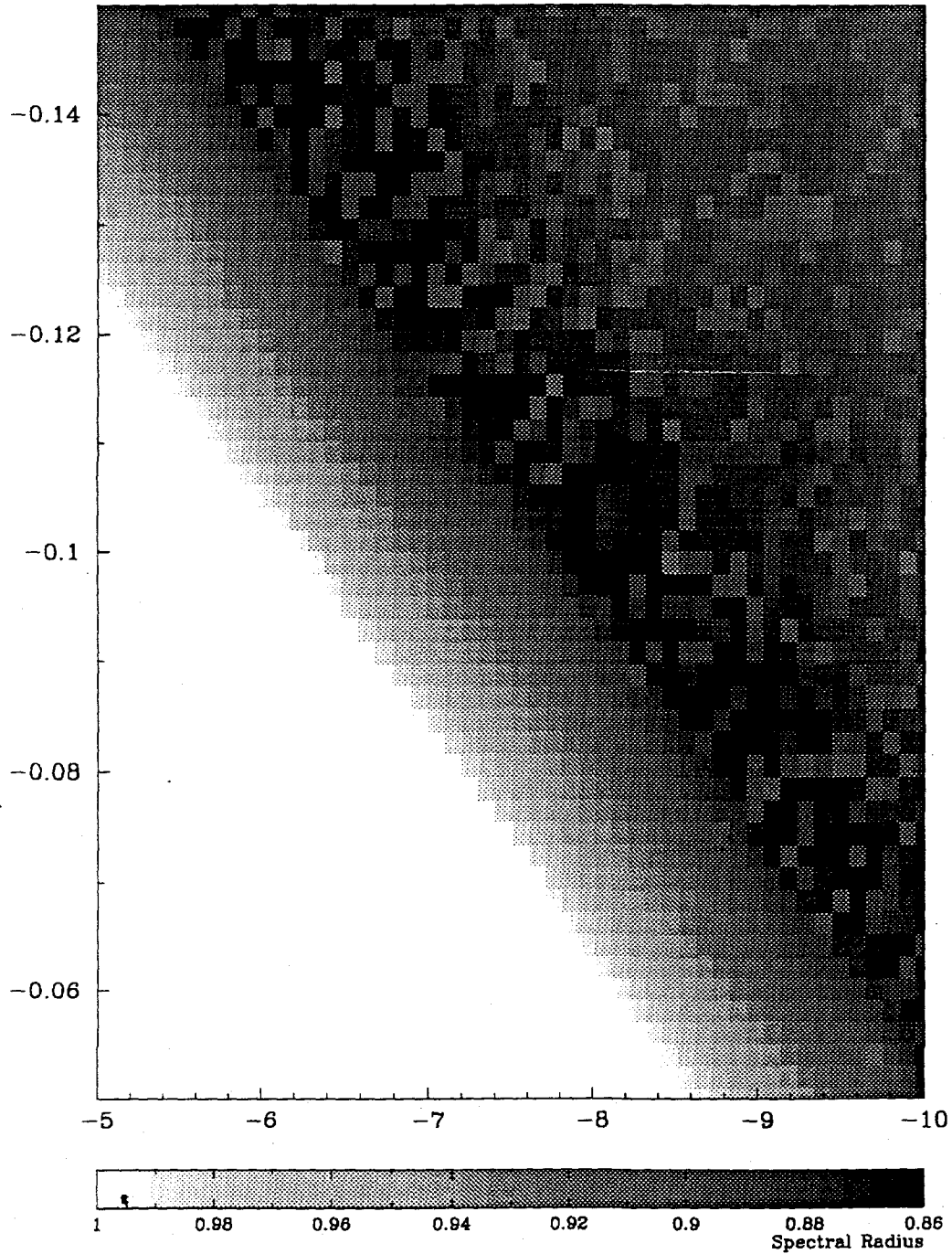
Conclusion

Deterioration in performance of the Adjacent-cell Preconditioner (AP), as well as other acceleration schemes, was observed in cases of Burre's Suite of Test Problems (BSTeP) characterized by sharp material discontinuity, i.e. large difference in total cross section. This phenomenon contradicts results of the spectral analysis of homogeneous-material model configurations. In order to incorporate material discontinuity in a model problem that can be analyzed we developed the Periodic Horizontal Interface (PHI) problem configuration and used it to investigate the performance of transport iterative schemes. This enabled us to demonstrate the inadequacy of the reciprocal averaging mixing formula across sharp material heterogeneities. Hence we used an optimization routine to numerically calculate values of the preconditioner elements that minimize the spectral radius of the AP iterations for a variety of problem settings. Our preliminary conclusion is that no cell-centered AP is unconditionally *robust*, meaning that no choice of the preconditioner parameters can be found that will keep the spectral radius bounded far below unity for arbitrary magnitude of the material discontinuity. Numerical experiments with edge-centered Diffusion Synthetic Acceleration (DSA) suggests similar deterioration in performance. Novel preconditioners that have nontraditional cell-coupling schemes that preclude this undesirable behavior are being sought.

References

1. W. A. Rhoades and D. B. Simpson, "The TORT Three-Dimensional Discrete Ordinates Neutron/Photon Transport Code," *ORNL/TM-13221*, to be published.
2. E. M. Gelbard and L. A. Hageman, "The Synthetic Method as Applied to the S_n Equations," *Nucl. Sci. Eng.*, **37**, 288 (1969).
3. W. H. Reed, "The Effectiveness of Acceleration Techniques for Iterative Methods in Transport Theory," *Nucl. Sci. Eng.*, **45**, 245 (1971).

Fig. 2. Spectral Radius of the AP Iterations for the PHI Configuration Over the D_{xj} Plane with $D_{yj} = -28752, -596.6$ for ONIM with S_4 Angular Quadrature, $C=I$, $a=1$, $b_1=b_2=.01$, and $\sigma_1=.01$, $\sigma_2=10$



4. R. E. Alcouffe, "Diffusion Synthetic Acceleration Methods for the Diamond-Differenced Discrete Ordinates Equations," *Nucl. Sci. Eng.*, **64**, 344 (1977).
5. E. W. Larsen, "Unconditionally Stable Diffusion Synthetic Acceleration Methods for the Slab Geometry Discrete Ordinates Equations. Part I: Theory," *Nucl. Sci. Eng.*, **82**, 47 (1982).
6. Y. Y. Azmy, "Cell-Centered Imposed Diffusion Synthetic Acceleration for Weighted Diamond Difference Methods," *Nucl. Sci. Eng.*, **115**, 265 (1993).
7. Y. Y. Azmy, "Adjacent-cell Preconditioners for Solving Optically Thick Neutron Transport Problems," in *Proc. Eighth Int. Conf. on Radiation Shielding*, Arlington, Texas, April 24-27, 1994, Vol. I, p. 193, American Nuclear Society, La Grange Park, Illinois (1994).
8. Y. Y. Azmy, "Adjacent-cell Preconditioners for Accelerating Multidimensional Neutron Transport Methods," in *Advances and Applications in Radiation Protection and Shielding*, N. Falmouth, MA, April 21-25, 1996, Vol. 1, p. 390, American Nuclear Society, La Grange Park, Illinois (1996).
9. R. E. Alcouffe, R. S. Baker, F. W. Brinkley, D. R. Marr, R. D. O'Dell, and W. F. Walters, "DANTSYS: A diffusion accelerated neutral particle transport code system," *LANL-12969*, 1995.
10. Thomas H. Rowan, "Functional Stability Analysis of Numerical Algorithms," PhD Thesis, University of Texas at Austin (1990).